ARTICLE

# Effects of Shape of Crowders on Dynamics of a Polymer Chain Closure

Bai-cheng Xia, Dong-hua Zhang, Jia-jun Wang, Wan-cheng Yu*

*CAS Key Laboratory of Soft Matter Chemistry, Department of Polymer Science and Engineering, University of Science and Technology of China, Hefei 230026, China*

(Dated: Received on March 1, 2017; Accepted on April 17, 2017)

Using 3D Langevin dynamics simulations, we investigate the effects of the shape of crowders on the dynamics of a polymer chain closure. The chain closure in spherical crowders is dominated by the increased medium viscosity so that it gets slower with the increasing volume fraction of crowders. By contrast, the dynamics of chain closure becomes very complicated with increasing volume fraction of crowders in spherocylindrical crowders. Notably, the mean closure time is found to have a dramatic decrease at a range of volume fraction of crowders 0.36−0.44. We then elucidate that an isotropic to nematic transition of spherocylindrical crowders at this range of volume fraction of crowders is responsible for the unexpected dramatic decrease in the mean closure time.

**Key words:** Loop formation, Crowding effects, Shape polydispersity

## I. INTRODUCTION

The process when two monomers separated by a large distance along the polymer chain come close enough to start interacting with each other is called loop formation. Loop formation of a polymer chain has been studied widely by experiments, theory, and simulations due to its great biological relevance [1–45]. For instance, the loop formation of DNA in the cell nucleus induced by transcription factor proteins makes sites of DNA separated by several μm on the genetic map be in molecular contact [1]. Another example is the contact formation of polypeptide chains which is considered as a basic step of protein folding [2]. Apart from its prevalence in biological systems, loop formation also exists widely in chemical systems, such as in telechelic polymers [3] and in carbon nanotudes [4].

So far, many specific aspects affecting the dynamics of a chain closure have been discussed, including the chain stiffness [5–7], the Coulomb interactions [8], the confinement effects [9], the complex chain relaxation [10, 11], and the excluded volume effects [12–17]. Due to its close biological relevance, how loop formation occurs in realistic cellular environments is an intriguing issue. The cellular environment in living biological cells is highly crowded and filled with a plenty of biomacromolecules, such as proteins, ribosomes, lipids, and cytoskeleton fibers. The volume fraction of these contents can be as large as 40%. It has been recognized in recent years that the crowded cellular environments could affect many biological processes, including gene expression and protein folding, *etc.* It is without doubt that an investigation about the dynamics of a polymer chain closure in crowded environments is of significant importance and meaning. Indeed, several advances in this aspect have been achieved recently [41–45]. Toan *et al.* [43] have studied the looping kinetics of self-avoiding polymers in crowded media and found that looping is entropically aided by the depletion effect while the increased friction impedes the diffusive encounter of the chain ends. The interplay of the depletion effect and the increased friction makes the looping of short chains slower and that of long chains faster [43]. Lately, Shin *et al.* [44] have reported how the crowder size affects the kinetics of polymer looping and showed that the loop formation gets slower in small crowders while it is accelerated in big crowders. More recently, they have investigated the polymer looping in crowded solutions of active particles and found that the presence of active particles yields a higher effective temperature of the bath so that the looping is facilitated [45].

It has been suggested by Kondrat *et al.* [46] that the polydispersity of the size of crowders has a striking effect on the diffusivity of macromolecules. At the same volume fraction of crowders, the chain diffusivity was shown to be slower with an increasing content of the small crowder in the composition [46]. Meanwhile, Kang *et al.* [47] reported that the polydispersity of the shape of crowders affects the conformational properties of semiflexible chains significantly. Obviously, the chain diffusivity and the chain conformational properties are closely related to the dynamics of a chain closure. However, up to now, how the polydispersity of the size and the shape of crowders affect the dynamics of a chain closure remains unclear. Therefore, by using three-dimensional (3D) Langevin dynamics simulations, we investigate in this work the dynamics of a

*Author to whom correspondence should be addressed. E-mail: ywcheng@ustc.edu.cn

DOI:10.1063/1674-0068/30/cjcp1703024 

chain closure in crowded environments where two different shapes of crowders, *i.e.*, the spherical and spherocylindrical crowders are introduced into the system. Note that the effects of the polydispersity of the size of crowders on the dynamics of a chain closure is not the subject of the present work.

## II. MODEL AND METHODS

The polymer in the simulations is modeled as a bead-spring chain [48]. Each bead in the chain represents a segment. The finite extension nonlinear elastic (FENE) potential is applied between neighboring beads along the chain to achieve their connections described by the spring. Here, the FENE potential is given as

$$U_{\rm FENE}(r) = -\frac{1}{2}kR_0{}^2\ln(1-\frac{r^2}{R_0^2}) \tag{1}$$

where $r$ is the distance between consecutive beads, $k$ is the spring constant and $R_0$ is the maximum allowed separation between connected beads. The repulsive non-bonded interactions between chain beads are modeled by the truncated Lennard-Jones (LJ) potential, namely the Weeks-Chandler-Andersen (WCA) potential [49]

$$U_{\rm WCA}(r) = \begin{cases} 4\varepsilon\left[\left(\frac{\sigma}{r}\right)^{12}-\left(\frac{\sigma}{r}\right)^{6}+\frac{1}{4}\right], & r\le 2^{1/6}\sigma \\ 0, & r>2^{1/6}\sigma \end{cases} \tag{2}$$

Here, $\sigma$=1 is the diameter of a chain bead, $r$ is the distance between beads, and $\varepsilon$=1 is the interaction strength between beads.

In order to mimic the crowding environments in realistic cells, crowders with different shapes are introduced into the cubic simulation box of a size $L_0$=15$\sigma$. As shown in FIG. 1, two different shapes of crowders are considered in the present work, *i.e.*, spherical (S-type) crowders and spherocylindrical (SC-type) crowders. The diameter of a S-type crowder is $\sigma$. The SC-type crowders are formed by connecting 5 spherical crowders together through the above FENE potential and a bending potential between successive bonds is applied

$$U_{\rm bend}(\theta) = \frac{\kappa}{2}(\theta-\theta_0)^2 \tag{3}$$

Here, $\theta$ is the angle between adjacent bond vectors with its equilibrium value $\theta_0$ being set to be $\pi$, and $\kappa$=1200 is the bending constant. Therefore, the SC-type crowder in our simulations can hardly bend and behave like a rod. The interactions between chains beads and two kinds of crowders are purely repulsive, which can also be described by the above WCA potential.

In the simulations, the motions of chain beads, S-type crowders and beads in SC-type crowders are described by the Langevin equation [50]:

$$m\ddot{\mathbf{r}}_i = -\nabla U_i - \xi\mathbf{v}_i + \mathbf{F}_i^R \tag{4}$$

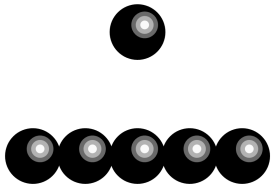

FIG. 1 Schematic illustration of the spherical and spherocylindrical crowders used in the simulations. The diameter of the spherical crowder is $\sigma$, and the spherocylindrical crowder is constructed by connecting 5 spherical crowders.

where $m$ is the bead's mass, $\xi$ is the friction coefficient of a bead, $\mathbf{v}_i$ is the bead's velocity. For chain beads, $U_i$=$\sum_{i\neq j}U^{ij}_{\rm WCA}$+$U_{\rm FENE}(i-1,i,i+1)$. For S-type crowders, $U_i$=$\sum_{i\neq j}U^{ij}_{\rm WCA}$. For beads in SC-type crowders, $U_i$=$\sum_{i\neq j}U^{ij}_{\rm WCA}$+$U_{\rm FENE}(i-1,i,i+1)$+$U_{\rm bend}(\theta_i)$. $-\nabla U_i$ and $-\xi\mathbf{v}_i$ is the conservative, frictional forces exerted on the $i$th bead, respectively. $\mathbf{F}_i^R$ is the random force satisfying the fluctuation-dissipation theorem [51]. The system energy, length and mass scales are determined by the LJ parameters $\varepsilon$, $\sigma$ and bead mass $m$, leading to the corresponding time scale $t_{\rm LJ}$=$(m\sigma^2/\varepsilon)^{1/2}$ which is order of ps. The reduced parameters for all simulations in this work are chosen to be $R_0$=2, $k$=7, and the temperature $T$=1.2. Then the Langevin equation is integrated in time by the method proposed by Ermak and Buckholzs [52] with the time step $\Delta t$=5×10$^{-3}$.

Initially, a polymer chain of the length $N$=20 and a set number of crowders $N_{\rm c}$ are introduced into a cubic simulation box of a much larger size $L$=10$L_0$. $N_{\rm c}$ is first estimated according to a pre-specified volume fraction of crowders $\phi_0$ and then obtained by rounding. In this way, the placement of crowders becomes much easier. Note that the periodic boundary conditions are applied in all directions. Then, the simulation box begins to contract gradually till its size equals to $L_0$. During the contraction process, the thermal relaxation of the chain and crowders described by the Langevin thermostat proceeds simultaneously. As the contraction process completes, the thermal relaxation continues for 5×10$^3$ $t_{\rm LJ}$. To ensure sufficient equilibration of the system, we have calculated the autocorrelation function of the end-to-end vector $c(t)$,

$$c(t) = \frac{\langle\mathbf{R}(t)\cdot\mathbf{R}(0)\rangle}{\langle\mathbf{R}(0)\cdot\mathbf{R}(0)\rangle} \tag{5}$$

Here, $\mathbf{R}(t)$ and $\mathbf{R}(0)$ is the end-to-end vector at time $t$ and 0, respectively. $c(t)$ is an exponential decay function of the time $t$. By fitting $c(t)$-$t$ curves at a range of $c(t)$=$[1,e^{-2}]$ in a semilogarithmic plot, the autocorrelation time $\tau_{\rm a}$ could be obtained from the negative reciprocals of the slopes of fitting linear lines directly. As shown in FIG. 2, the autocorrelation time $\tau_{\rm a}$ at $\phi$=0,

DOI:10.1063/1674-0068/30/cjcp1703024 

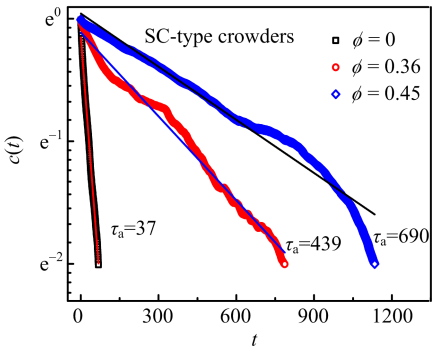


FIG. 2 The autocorrelation function of the end-to-end vector of a polymer chain in SC-type crowders $c(t)$ as a function of the time $t$ under three different volume fractions of crowders $\phi$=0, 0.36, and 0.45. The solid lines are the linear fittings to the data.

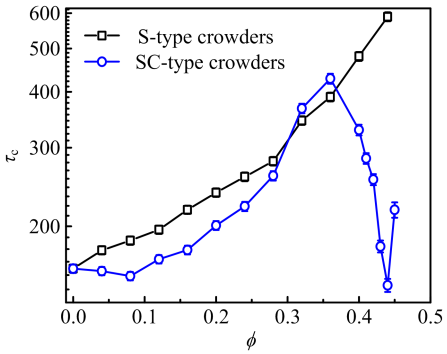


FIG. 3 Dependence of the mean closure time $\tau_c$ on the volume fraction of crowders $\phi$. Here, the crowders have two different shapes, *i.e.*, the S-type and SC-type crowders.

0.36 and 0.45 is 37, 439, and 690, respectively. These $\tau_a$ are much shorter than the thermal relaxation time $5\times10^3$ $t_{LJ}$ in the simulations so that the the system is actually equilibrated even for the highest volume fraction of crowders $\phi$=0.45 we have studied. With all of these done, the chain dynamics is monitored till its two end segments are within a capture radius $a$=2.5$\sigma$, *i.e.*, a closure event completes. The closure time $t_c$ is identified with the first passage time of the searching process of the two end segments. Each datum point reported in this work is derived from averaging over 2000 independent runs so as to reduce statistical errors. The mean closure time $\tau_c$ is an average of 2000 closure times $t_c$.

## III. RESULTS AND DISCUSSION

The process of a polymer chain closure is a conformational transition from the states that the chain with an end-to-end distance $R_{ee}>a$ to the state $R_{ee}=a$. In realistic cells, the conformational transitions of biopolymers, such as proteins, take place in crowded environment. The presence of crowders leads to an increased medium viscosity. Meanwhile, non-ignorable depletion attractions between chain segments emerge. Obviously, the increased medium viscosity impedes the contact of the two end beads of the chain as its conformational transition could be considered as a diffusive process of barrier crossing according to the Kramers theory [53]. However, the depletion attractions compress the conformational space of the chain and thus facilitate the chain closure. The interplay of these two favorable and unfavorable factors for the chain closure process resulting from the crowding effects determines how the dynamics of chain closure depends on the volume fraction of crowders $\phi$.

It has been suggested by Shin *et al.* [44] that the size of crowders could determine the outcome of this interplay. Specifically, the chain closure gets slower in small crowders as the increased medium viscosity dominates; while it becomes faster in big crowders due to the prevailing confinement effects. We noted that the shape of crowders could affect the conformational transitions of semiflexible polymer chains significantly [47]. For flexible chains, this factor should also play an important role in the conformational transitions of chains and the dynamics of chain closure investigated here. Therefore, we have performed a set of simulation contrast tests to examine how the shape of crowders affects the dynamics of chain closure.

The core result of this work is presented in FIG. 3. When the crowders in the system are spherical, the mean closure time $\tau_c$ increases monotonically with the increasing volume fraction of crowders $\phi$. This observation is due to the dominating increased medium viscosity during the chain closure and is consistent with the work of Shin *et al.* [44]. By comparison, for SC-type crowders, the dynamics of chain closure gets much more complicated as $\phi$ increases and can be roughly divided into four dynamic regimes. For $\phi\leq$0.08, a slight decline in $\tau_c$ is observed. With a further increase in $\phi$, $\tau_c$ increases sharply till $\phi$=0.36. Afterwards, a dramatic decrease in $\tau_c$ emerges and the chain closure at $\phi$=0.44 is even faster than that at $\phi$=0. Finally, a sharp increase in $\tau_c$ appears again.

The complicated dynamic behaviors of chain closure that proceed in SC-type crowders reflect the complexity of the interplay between the unfavorable increased medium viscosity and the favorable compressed conformational space in this case. The strength of the depletion attractions induced by the presence of S-type crowders is $\approx\phi k_BT/\sigma^2$. However, this strength is $\approx\phi Pk_BT/\sigma^2$ for SC-type crowders with $P$ being the length of SC-type crowders [47]. Therefore, a polymer chain in SC-type crowders is likely to be more compact than the one in S-type crowders at the same $\phi$. As shown in FIG. 4, the mean squared end-to-end distance of a chain in SC-type crowders $\langle R_{ee}\rangle$ is always smaller than that of a chain in S-type crowders at the same $\phi$. When the increased medium viscosity induced by the presence of crowders is not very striking at low $\phi$, the

DOI:10.1063/1674-0068/30/cjcp1703024 

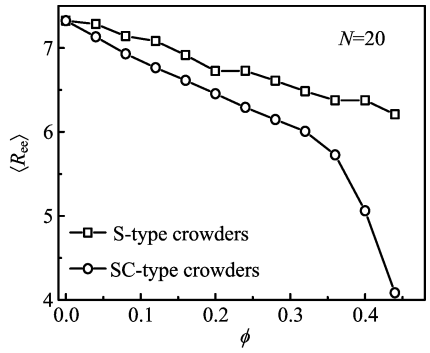


FIG. 4 The mean squared end-to-end distance of a polymer chain $\langle R_{\rm ee}\rangle$ as a function of the volume fraction $\phi$ of two kinds of shapes of crowders.

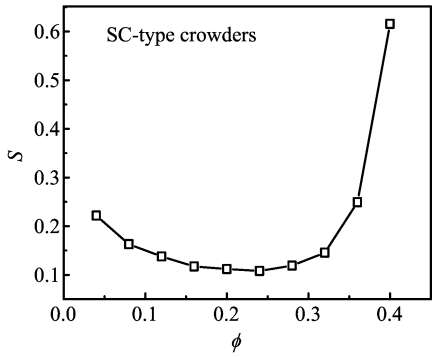


FIG. 5 The nematic order parameter $S$ of SC-type crowders as a function of $\phi$.

smaller $\langle R_{\rm ee}\rangle$ of a chain in SC-type crowders accounts for the slight decline in $\tau_{\rm c}$. As $\phi$ increases further, the increased medium viscosity dominates the dynamics of chain closure so that a sharp increase in $\tau_{\rm c}$ is observed. In contrast to the gradual decrease in $\langle R_{\rm ee}\rangle$ of a chain in S-type crowders at the whole range of $\phi$ we have measured, the chain in SC-type crowders undergoes a dramatic decrease in its size at $\phi$=0.36−0.44 as plotted in FIG. 4. This observation provides a phenomenological explanation about the significantly accelerating chain closure at the corresponding range of $\phi$. However, what is the underlying physical origin of the dramatic decrease in $\langle R_{\rm ee}\rangle$ at $\phi$=0.36−0.44?

Unlike the isotropic S-type crowders, the SC-type crowders in this work have an aspect ratio $\delta=\frac{P}{\sigma}\approx 5$ and are highly anisotropic. According to the Onsager theory [54], the rod-like SC-type crowders may undergo an isotropic to nematic ($I$-$N$) transition with increasing $\phi$. To clarify whether the $I$-$N$ transition would occur as $\phi$ increases to a certain range, we have calculated the nematic order parameter of the SC-type crowders which is defined as

$$S=\frac{1}{N_{\rm c}}\sum_{i=1}^{N_{\rm c}}\frac{3\cos^2\theta_i-1}{2} \tag{6}$$

where $\theta_i$ is the orientational angle of the $i$th SC-type crowder. In the simulations, the nematic order parameter $S$ is calculated by solving the largest eigenvalue of the ordering matrix $\mathbf{Q}$. $\mathbf{Q}$ is defined in the terms of the orientations of the crowder axes $\mathbf{u_i}$ [55]

$$\mathbf{Q}=\frac{1}{N_{\rm c}}\sum_{i=1}^{N_{\rm c}}\left(\frac{3}{2}\mathbf{u_i}\mathbf{u_i}-\frac{\mathbf{I}}{2}\right) \tag{7}$$

Here $\mathbf{I}$ is the unit tensor. The value of the nematic order parameter $S$ is close to zero in the isotropic phase, while it approaches to one in the nematic phase.

As shown in FIG. 5, an initial decrease in $S$ followed by a stable value of $S$ is observed due to a small quantity of SC-type crowders. However, $S$ increases dramatically as $\phi\geq$0.32 which is indicative of the $I-N$ transition. Concomitantly, the polymer chain is confined among SC-type crowders so that a sharp decrease in its $\langle R_{\rm ee}\rangle$ occurs. This similar caging effect on a polymer chain has also been reported by Shin *et al.* [44]. The difference lies in that the caging effect here is a result of the $I$-$N$ transition of SC-type crowders, while in the work of Shin *et al.* [44], this effect is just caused by the size of crowders. In addition, both the strength of the depletion attraction induced by SC-type crowders and their excluded volume interactions depend on the size of a SC-type crowder. If the size of the monomer of a SC-type crowder decreases, the strength of the depletion attraction is expected to get enhanced, while the excluded volume interactions is weakened. As a consequence, there might be a more obvious decrease in $\tau_{\rm c}$ at low $\phi$, and the accelerating effect of the chain closure due to the $I$-$N$ transition of SC-type crowders at high $\phi$ might be less pronounced. Nonetheless, the four dynamic regimes of chain closure that proceeds in SC-type crowders would be retained.

## IV. CONCLUSIONS

We have investigated the effects of the shape of crowders on the dynamics of a polymer chain closure by using 3D Langevin dynamics simulations in the present work. We show that the chain closure in spherical crowders gets slower with the increasing volume fraction of crowders $\phi$, which is simply due to the dominating increased medium viscosity. By contrast, the dynamics of chain closure becomes very complicated with increasing $\phi$ in spherocylindrical crowders. Notably, the mean closure time $\tau_{\rm c}$ is found to have a dramatic decrease at a range of $\phi$=0.36−0.44 in this case. The superficial reason is the much more rapid decrease in the mean squared end-to-end distance of a chain in spherocylindrical crowders at this range of $\phi$ compared with the case of spherical crowders. By calculating the nematic order parameter $S$ of spherocylindrical crowders, we find that the crowders in the system undergo an

DOI:10.1063/1674-0068/30/cjcp1703024 

isotropic to nematic transition with increasing $\phi$. It is the occurrence of this transition that gives rise to the striking caging effects suffered by the polymer chain. In view of the complexity of the crowded cellular environments, our results here are of great relevance to the loop formation of biopolymers in realistic cells.

## V. ACKNOWLEDGMENTS

This work is supported by the Fundamental Research Funds for the Central Universities of China (No.WK2060200020) and the China Postdoctoral Science Foundation (No.2015M581998).

[1] J. Allemand, S. Cocco, N. Douarche, and G. Lia, Eur. Phys. J. E **19**, 293 (2006).
[2] L. Lapidus, W. Eaton, and J. Hofrichter, Proc. Natl. Acad. Sci. USA **97**, 7220 (2000).
[3] Y. Sheng, P. Hsu, J. Z. Y. Chen, and H. Tsao, Macromolecules **37**, 9257 (2004).
[4] M. Sano, A. Kamino, J. Okamura, and S. Shinkai, Science **293**, 1299 (2001).
[5] S. Jun, J. Bechhoefer, and B. Ha, Europhys. Lett. **64**, 420 (2003).
[6] A. Dua and B. Cherayil, J. Chem. Phys. **116**, 399 (2002).
[7] R. Afra and B. Todd, J. Chem. Phys. **138**, 174908 (2013).
[8] J. Stample and I. Sokolov, J. Chem. Phys. **114**, 5043 (2001).
[9] P. Bhattacharyya, R. Sharma, and B. Cherayil, J. Chem. Phys. **136**, 234903 (2012).
[10] I. Sokolov, Phys. Rev. Lett. **90**, 080601 (2003).
[11] T. Guérin, O. Bénichou, and R. Voituriez, Nat. Chem. **4**, 568 (2012).
[12] A. Rey and J. Freire, Macromolecules **24**, 4673 (1991).
[13] (a) B. Friedman and B. O'Shaughnessy, Phys. Rev. A **40**, 5950 (1989);
(b) B. Friedman and B. O'Shaughnessy, Europhys. Lett. **23**, 667 (1993);
(b) B. Friedman and B. O'Shaughnessy, Macromolecules **26**, 4888 (1993);
(c) B. Friedman and B. O'Shaughnessy, Macromolecules **26**, 5726 (1993).
[14] A. Podtelezhnikov and A. Vologodskii, Macromolecules **30**, 6668 (1997).
[15] M. Ortiz-Repiso, J. Freire, and A. Rey, Macromolecules **31**, 8356 (1998).
[16] J. Kim and S. Lee, J. Chem. Phys. **121**, 12640 (2004).
[17] J. Kim, W. Lee, J. Sung, and S. Lee, J. Phys. Chem. B **112**, 6250 (2008).
[18] (a) G. Wilemski and M. Fixman, J. Chem. Phys. **60**, 866 (1974);
(b) G. Wilemski and M. Fixman, J. Chem. Phys. **60**, 878 (1974).
[19] M. Doi, Chem. Phys. **9**, 455 (1975).
[20] A. Szabo, K. Schulten, and Z. Schulten, J. Chem. Phys. **72**, 4350 (1980).
[21] A. Ansari, C. Jones, E. Henry, J. Hofrichter, and W. Eaton, Science **256**, 1796 (1992).
[22] H. Neuweiler, M. Löllmann, S. Doose, and M. Sauer, J. Mol. Biol. **365**, 856 (2007).
[23] A. Möglich, F. Krieger, and T. Kiefhaber, J. Mol. Biol. **345**, 153 (2005).
[24] M. Buscaglia, L. Lapidus, W. Eaton, and J. Hofrichter, Biophys. J. **91**, 276 (2006).
[25] J. Fernández, A. Rey, J. Freire, and I. de Piérola, Macromolecules **23**, 2057 (1990).
[26] S. Chan and K. Dill, J. Chem. Phys. **90**, 492 (1989).
[27] P. Debnath and B. Cherayil, J. Chem. Phys. **120**, 2482 (2004).
[28] N. Toan, G. Morrison, C. Hyeon, and D. Thirumalai, J. Phys. Chem. B **112**, 6094 (2008).
[29] J. Z. Y. Chen, H. Tsao, and Y. Sheng, Phys. Rev. E **72**, 031804 (2005).
[30] D. Doucet, A. Roitberg, and S. Hagen, Boiphys. J. **92**, 2281 (2007).
[31] I. Yeh and G. Hummer, J. Am. Chem. Soc. **124**, 6563 (2002).
[32] T. Uzawa, T. Isoshima, Y. Ito, K. Ishimori, and D. Makarov, and K. Plaxco, Boiphys. J. **104**, 2485 (2013).
[33] W. Yu and K. Luo, Sci. China Chem. **58**, 689 (2015).
[34] W. Yu and K. Luo, J. Chem. Phys. **142**, 124901 (2015).
[35] D. Sarkar, S. Thakur, Y. Tao, and R. Kapral, Soft Matter **10**, 9577 (2014).
[36] R. Everaers and A. Rosa, J. Chem. Phys. **136**, 014902 (2012).
[37] A. Amitai, I. Kupka, and D. Holcman, Phys. Rev. Lett. **109**, 108302 (2012).
[38] A. Amitai and D. Holcman, Phys. Rev. Lett. **110**, 248105 (2013).
[39] L. Lapidus, P. Steinbach, W. Eaton, A. Szabo, and J. Hofrichter, J. Phys. Chem. B **106**, 11628 (2002).
[40] H. Neuweiler, A. Schulzn, M. Böhmer, J. Enderlein, and M. Sauer, J. Am. Chem. Soc. **125**, 5324 (2003).
[41] O. Stiehl, K. Weidner-Hertrampf, and M. Weiss, New J. Phys. **15**, 113010 (2013).
[42] J. Shin, A. G. Cherstvy, and R. Metzler, ACS Macro Lett. **4**, 202 (2015).
[43] N. Toan, D. Marenduzzo, P. Cook, and C. Micheletti, Phys. Rev. Lett. **97**, 17830 (2006).
[44] J. Shin, A. G. Cherstvy, and R. Metzler, Soft Matter **11**, 472 (2015).
[45] J. Shin, A. G. Cherstvy, W. K. Kim, and R. Metzler, New J. Phys. **17**, 113008 (2015).
[46] S. Kondrat, O. Zimmermann, W. Wiechert, and E. von Lieres, Phys. Biol. **12**, 046003 (2015).
[47] H. Kang, N. M. Toan, C. Hyeon, and D. Thirumalai, J. Am. Chem. Soc. **137**, 10970 (2015).
[48] K. Kremer and G. Grest, J. Chem. Phys. **92**, 5057 (1990).
[49] J. D. Weeks, D. Chandler, and H. C. Andersen, J. Chem. Phys. **54**, 5237 (1971).
[50] M. P. Allen and D. J. Tildesley, *Computer Simulation of Liquids* New York: Oxford University Press, (1987).
[51] D. Chandler, *Introduction to Modern Statistical Mechanics*, New York: Oxford University Press, (1987).
[52] D. L. Ermak and H. Buckholz, J. Comput. Phys. **35**, 169 (1980).
[53] P. Hänggi, P. Talkner, and M. Borkovec, Rev. Mod. Phys. **62**, 251 (1990).
[54] L. Onsager, Ann. N. Y. Acad. Sci. **51**, 627 (1949).
[55] S. C. McGrother, D. C. Williamson, and G. Jackson, J. Chem. Phys. **104**, 6755 (1996).

DOI:10.1063/1674-0068/30/cjcp1703024 